Thermodynamics of Electron Transfer in Oxygenic Photosynthetic Reaction Centers: Volume Change, Enthalpy, and Entropy of Electron-Transfer Reactions in the Intact Cells of the Cyanobacterium *Synechocystis* PCC 6803†

Vladimir A. Boichenko,‡,§ Jian-Min Hou,‡ and David Mauzerall*,‡

The Rockefeller University, 1230 York Avenue, New York, New York 10021, and Institute of Basic Biological Problems, Russian Academy of Sciences, 142290 Pushchino, Russia

Received August 31, 2000; Revised Manuscript Received April 19, 2001

ABSTRACT: The volume and enthalpy changes for charge transfer in the 0.1−10 μs time window in photosynthetic reaction centers of the intact cells of *Synechocystis* PCC 6803 were determined using pulsed, time-resolved photoacoustics. This required invention of a method to correct for the cell artifact at the temperature of maximum density of water caused by the heterogeneous system. Cells grown under either white or red light had different PS I/PS II molar ratios, ∼3 and ∼1.7, respectively, but invariable action spectra and effective antenna sizes of the photosystems. In both cultures, the photoacoustic measurements revealed that their thermodynamic parameters differed strongly in the spectral regions of predominant excitation of PS I (680 nm) and PS II (625 nm). On correcting for contribution of the two photosystems at these wavelengths, the volume change was determined to be -27 ± 3 and -2 ± 3 Å^3 for PS I and PS II, respectively. The energy storage on the ∼1 μs time scale was estimated to be 80 ± 15% and 45 ± 10% per trap in PS I and PS II, respectively. These correspond to enthalpies of -0.33 ± 0.2 and -1 ± 0.2 eV for the assumed formation of ion radical pairs $P_{700}{}^+F_{AB}{}^-$ and $Y_Z{}^\bullet P_{680}Q_A{}^-$, respectively. Taking the free energy of the above reactions as the differences of their redox potentials in situ, apparent entropy changes were estimated to be $+0.4 \pm 0.2$ and -0.2 ± 0.2 eV for PS I and PS II, respectively. These values are similar to that obtained in vitro for the purified reaction center complexes on the microsecond time scale [Hou et al. (2001) *Biochemistry 40*, 7109−7116, 7117−7125]. The constancy of these thermodynamic values over a 2-fold change of the ratio of PS I/PS II is support for this method of in vivo analysis. Our pulsed PA method can correct the "cell" or heterogeneous artifact and thus opens a new route for studying the thermodynamics of electron transfer in vivo.

In oxygenic photosynthetic organisms, the reaction centers of PS[1] I and PS II convert the absorbed light energy into stable biochemical products, i.e., reduced ferredoxin and oxygen (see reviews in refs *1*−*4*). This conversion involves a variety of electron-transfer reactions on different time scales. Thermodynamic properties of these steps can be investigated by pulsed, time-resolved photoacoustic spectroscopy (*5*), which was applied both to the primary processes of photosynthesis in the microsecond time window (*6*−*10*) and to the terminal charge stabilization on a time scale of milliseconds (*11*, *12*).

In the liquid phase, fast photoacoustic signals are sensitive not only to the enthalpy of photosynthetic electron-transfer reactions, detected by the thermal expansion of the solution, but also to the large negative (contraction) volume change of photochemical reaction centers (*13*−*17*). However, except for data from Delosme et al. (*9*, *10*), earlier photoacoustic studies (*6*−*8*) on oxygenic photosynthesis in the microsecond time window have neglected the contraction signal. This makes questionable the estimations of energy storage. In particular, the relative energy storage in PS I was found to be >70% in both the isolated particles (6) and intact cyanobacterial cells (*7*, *8*). This is significantly larger than the values of ∼58% and 52% calculated from the midpoint potential differences (a free energy) for states $P_{700}{}^+F_{AB}{}^-$ and $P_{700}{}^+Fd^-$, respectively. In contrast, Delosme et al. (*9*) have estimated that the charge separation in the PS I complex from *Synechocystis* is accompanied by a volume contraction of −20 Å^3 and energy storage of ∼55%. They did not determine the volume change for PS II. The data of Figure 5 in ref *9* implies a contraction of ∼−11 Å^3 for "DEAE" PS II from *Chlamydomonas reinhardtii*. However, their data on the energy storage differed greatly for different types of PS II particles.

Thus, to date, there is no complete and valid information about the in vivo thermodynamic properties of the photo-induced charge separation in PS I and PS II on the microsecond time scale.

† This work is supported by grants from the NSF (MCB 99-04522) and NIH (GM 25693).

* Corresponding author. Fax: (212) 327-8853. E-mail: mauzera@rockvax.rockefeller.edu.

‡ The Rockefeller University.

§ Russian Academy of Sciences.

[1] Abbreviations: ES, energy storage; F_{AB}, iron−sulfur clusters in photosystem I centers; PA, photoacoustics; PS, photosystem; P_{700}, photosystem I primary donor; Q_A, primary electron acceptor quinone in photosystem II; RC, reaction center; RL, red light; WL, white light; Y_Z, tyrosine-161 on subunit D1 of photosystem II.

10.1021/bi010374k CCC: $20.00
Published on Web 05/23/2001

In the present work, we report results of a global analysis of the photoacoustic data for the primary reactions of PS I and PS II in the intact cells of the cyanobacterium *Synechocystis* sp. PCC 6803 for comparison with the same parameters of isolated reaction complexes described in separate papers. This required corrections for both the cell artifact caused by the heterogeneous system and the relative excitation efficiency for PS I and PS II.

MATERIALS AND METHODS

Culture and Growth Conditions. Experiments were performed on 5−7-day-old cell cultures of *Synechocystis* sp. PCC 6803 incubated at 20 °C in shaken conic flasks with 200 mL of Kratz-Mayers C medium. Two different light regimes of altered spectral composition were used to change the PS I/PS II molar ratio. Light intensity was 15−20 μE m^{-2} s^{-1} under either a "cool white" fluorescent lamp or an incandescent lamp covered with a red transparency (the fraction of photosynthetically active radiation in the spectral region >650 nm was estimated to be ∼2% and 80%, respectively). The cultures had similar absorption spectra with the ratios of 0.95 ± 0.1 for optical density at 625 and 680 nm.

Functional Activity Measurements. Light-saturated rates of oxygen evolution in the presence of artificial electron acceptors and dark respiration rates in the cells were measured by a Clark electrode. Polarographic measurements of a microsecond flash-induced O_2 gas exchange related to photochemical activity of both PS II (O_2 evolution) and PS I (photoinhibition of respiration), and their action spectra and optical cross sections were performed using a bare platinum electrode as previously described (*18*, *19*). Assays of cells deposited on the surface of the rate electrode in 50 mM sodium phosphate buffer with 50 mM KCl, pH 6.8, had a chlorophyll equivalent layer density of ∼1 μg cm^{-2}. O_2 evolution with actinic light was recorded in the presence of a weak continuous illumination >700 nm. Photoinhibition of respiration was separately recorded in the presence of 10 μM diuron. Action spectra were recorded using the intermittent actinic illumination of 1 s light flashes with variable 20−60 s dark intervals. During scanning of the spectra, the spectral half-width of the monochromatic beam was 1−3 nm, and its intensity was below 0.2 nE cm^{-2} s^{-1}. Effective antenna sizes of the photosystems were calculated using the in situ values of an optical cross section for a single chlorophyll molecule, 2.3 ± 0.1 and 2.68 ± 0.04 A^3 in isolated PS I and PS II complexes from *Synechocystis* PCC 6803 at 675 and 680 nm, respectively.

Photoacoustic Apparatus. Photoacoustic (PA) measurements were carried out using samples of ∼0.15 optical density per mm at 675 nm in a 1 mm cell designed according to Arnaut et al. (*20*). The back side of the PA cell was assembled with a dielectric mirror (99% reflection for 600−700 nm, Newport) which was acoustically coupled to a 128 μm piezoelectric film via a stainless steel holder. A Nd:YAG laser (Surelite II, Continuum) and optical parametric oscillator with a red filter were used to produce 7 ns pulses of 625 or 680 nm light. The beam was focused through a 1 mm hole and recollimated on the cell following a 1.2 cm diameter iris. The light pulse energy from a beam pickoff was measured with a Molectron 2000 detector and J3-09 probe and was read by a computer HP 360 using the calibrated ratio to the light incident on the cell estimated with a J25LP-2 probe. The signal from the piezoelectric film was amplified by an Amtek preamplifier, filtered to pass 3 kHz/400 kHz, and further amplified by an Ithaco 1201 preamplifier before being digitized (Tektronix 710) and stored in the computer. The temperature of the cell was controlled to ±0.1 °C (Neslab RTE-5) using a type T thermocouple inserted in the brass cell holder and was also stored in the computer. Programs for analysis of data were written by D. Mauzerall.

Photoacoustic Measurements. An external calorimetric reference, which degrades absorbed photons to heat faster than the resolution time, was a carbon black ink adjusted to the same optical density as the sample at a given wavelength in the same buffer medium. The internal calorimetric reference for intact cyanobacterial cells was the heat emission by the closed photochemical reaction centers under strong (∼50 μE m^{-2} s^{-1}) background illumination. Low flux was used for excitation of samples because of the large optical cross section in vivo. The samples were often replaced in the PA cell during an experiment, and no change of PA signals was found.

The difficulty in the PA measurement of intact cells is the heterogeneous or "cell" artifact at the temperature of maximum density of near 4 °C described in the Results section. The following procedure allows us to obtain both the ΔV and ΔH, and thus the efficiency, of the photosynthetic system in vivo in the presence of the "cell artifact" of the heterogeneous sample. It requires five measurements instead of the usual three. One measures the PA signal of the cell suspension at temperature, T, and in the dark, D, with pulse energy low enough to obtain true efficiency: PA(cell,T,D) and another in background saturating light, S: PA(cell,T,S). The two measurements are repeated at the temperature of maximum density, near 4 °C: PA(cell,M,D) and PA(cell,M,S). The reference sample of the same absorbance is measured at temperature T to calibrate the scales: PA(ref,T). These measurements are

$$\mathrm{PA(ref,T)} = \frac{F_\mathrm{T}}{\kappa_\mathrm{T}}(E_\mathrm{A}\alpha_\mathrm{T} I(t)) \tag{1}$$

$$\mathrm{PA(cell,T,D)} = \frac{F_\mathrm{T}}{\kappa_\mathrm{T}}[E_\mathrm{D}(1 + \alpha(w,T,t))*\alpha(c,T,t) + V_\mathrm{T}]*I(t) \tag{2}$$

where F_T = piezo film sensitivity at temperature T, κ_T = compressibility of water at temperature T, and $\alpha(w,T,t$ or $c,T,t)$ refers to the complex thermal expansion/heat capacity times the density of the water or the cell cytoplasm, now a function of time (t) because of the thermal diffusion from cell to water with differing α's. Note that this does not occur in a homogeneous system because as thermal diffusion occurs into a larger volume, decreasing the temperature, the volume increases, keeping $\Delta V = \alpha V \Delta T$ constant. This is exact for a linear response. E_D refers to that fraction of the absorbed energy E_A that is emitted as heat. For simplicity we will assume that the responses are fast, i.e., within less than the response time of the system. $I(t)$ is the impulse response of the system. The symbol * refers to the convolution operation. It is also assumed that the small effects of differing κ's in

water and cells are negligible. In saturating background light:

$$\mathrm{PA(cell,T,S)} = \frac{F_\mathrm{T}}{\kappa_\mathrm{T}}[E_\mathrm{A}(1 + \alpha(w,T,t))^*\alpha(c,T,t)]^*I(t) \quad (3)$$

At the temperature of maximum density, M, the term $\alpha(w,T,t)$ is zero and the equations for PA(cell,M,D or cell,M,S) are the above without this term. Upon normalizing to the reference sample, the equations become

$$\mathrm{PA'(cell,T,D)} = \frac{E_\mathrm{D}}{E_\mathrm{A}}(1 + \alpha'(w,T,t))^*\alpha'(c,T,t) + \frac{V_\mathrm{T}}{E_\mathrm{A}\alpha_\mathrm{T}} \quad (4)$$

$$\mathrm{PA'(cell,T,S)} = (1 + \alpha'(w,T,t))^*\alpha'(c,T,t) \quad (5)$$

$$\mathrm{PA'(cell,M,D)} = \frac{F_\mathrm{M}\kappa_\mathrm{T}E_\mathrm{D}}{F_\mathrm{T}\kappa_\mathrm{M}E_\mathrm{A}}\alpha'(c,M,t) + \frac{V_\mathrm{M}}{E_\mathrm{A}\alpha_\mathrm{T}} \quad (6)$$

$$\mathrm{PA'(cell,M,S)} = \frac{F_\mathrm{M}\kappa_\mathrm{T}}{F_\mathrm{T}\kappa_\mathrm{M}}\alpha'(c,M,t) \quad (7)$$

where α' refers to the convolution of the time-dependent α's with the impulse response and normalized to α of water at T. It is seen that, assuming $V_\mathrm{T} = V_\mathrm{M}$:

$$\frac{E_\mathrm{D}}{E_\mathrm{A}} = \frac{\mathrm{PA'(cell,T,D)} - \mathrm{PA'(cell,M,D)}}{\mathrm{PA'(cell,T,S)} - \mathrm{PA'(cell,M,S)}} \quad (8)$$

$$\frac{V}{E_\mathrm{A}\alpha_\mathrm{T}} = \mathrm{PA'(cell,T,D)} - \frac{E_\mathrm{D}}{E_\mathrm{A}}\mathrm{PA'(cell,T,S)} \quad (9)$$

Thus the efficiency and the reaction volume are obtained directly from the five measurements with no assumptions of how the $\alpha(t)$'s vary with temperature or time.

Absorbance Spectrometry. Absorption spectra were recorded using an Aminco DW2000 spectrophotometer with an opal glass between the detector and closely placed sample to minimize distortion due to light scattering. Chlorophyll concentration in the cells was estimated using the extinction coefficients of Porra et al. (*21*) following extraction in dimethylformamide.

RESULTS

Synechocystis cultures were grown under lights of two different spectral compositions, changing the PS I/PS II molar ratio (*22*). As shown in Table 1, the red light (RL) grown cells had a 1.5 times increased maximum O_2 evolution rate in the presence of artificial electron acceptors and a 1.5 times decreased dark endogenic respiration rate compared to the white light (WL) grown cells. The flash yield measurements of PS II-mediated O_2 evolution and PS I-mediated photoinhibition of respiration indicated a virtually invariable content of the competent PS II reaction centers but a selective 2-fold decrease of the content of competent PS I reaction centers in the RL-grown culture compared to the WL-grown culture. Such change in the photosystem stoichiometry is a common phenomenon for many species of cyanobacteria (*23*). There was only a small ~15% increase of the effective phycobilin antenna of PS II in RL-grown cells as shown from the comparison of σ_{625} for the cultures (Table 1). In contrast, both the effective chlorophyll antenna sizes and action spectra of PS I and PS II units were virtually invariable by the different light regimes (Table 1, Figure 1). Taking into account the PS I/PS II ratio and their optical cross sections, we calculated a relative spectral efficiency of the photosystem excitation in two cultures (Figure 2). The spectra showed predominant excitation of PS II at the 625 nm band of phycocyanin and predominant excitation of PS I at the 680 nm band of chlorophyll that was used to discriminate activity of the two photosystems in our PA measurements.

Even at room temperature low energy (~1 μJ/cm^2) trains of laser pulses produced negative (contractive) photoacoustic signals in the microsecond time window from the competent reaction centers in intact cells of *Synechocystis* (Figure 3). In contrast, positive (expansive) signals were observed from

Table 1: Functional Characteristics of *Synechocystis* PCC 6803 Cells Grown under White Light (WL) or Red Light (RL)[a]

parameter	WL-grown cells	RL-grown cells
O_2 evolution rate, μmol (mg of Chl)$^{-1}$ h^{-1}	122 ± 10[b]	185 ± 20[b]
O_2 uptake dark rate, μmol (mg of Chl)$^{-1}$ h^{-1}	12 ± 2	7 ± 2
RC I/Chl, au	1[c]	0.48[c]
RC II/Chl, au	0.34[d]	0.28[d]
RC I/RC II	2.92	1.71
σ_{680} (PS I activity), Å^2	196 ± 10[c]	188 ± 10[c]
σ_{625} (PS II activity), Å^2	425 ± 20[d]	515 ± 30[d]
N_I, chlorophylls	85 ± 5[c]	82 ± 5[c]
N_II, chlorophylls	44 ± 5[d]	48 ± 5[d]

[a] Representative data or when shown are the averages ± SE for n = 3. [b] O_2 evolution rate was measured at white light of ~400 μE cm^{-2} s^{-1} in the presence of 0.2 mM dichlorobenzoquinone/1 mM ferricyanide. [c] Relative content of competent reaction centers (RC), effective optical cross section σ, and effective antenna size N for PS I were calculated from light saturation curves of photoinhibition of respiratory O_2 uptake (in the presence of 10 μM diuron) upon one-turnover flashes. [d] The same parameters for PS II were calculated from flash-induced O_2 evolution yields under continuous weak background illumination at >700 nm.

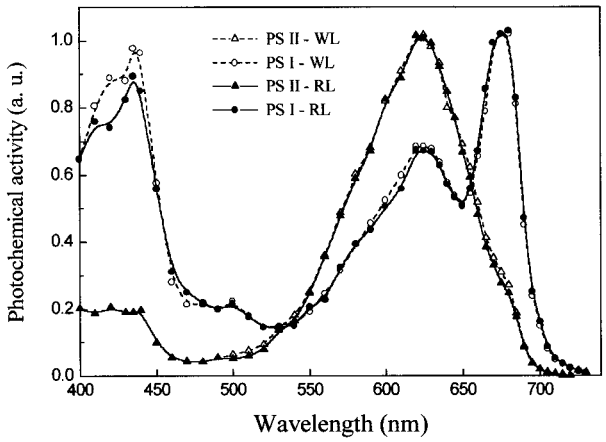

FIGURE 1: Action spectra of PS I and PS II activity in WL- and RL-grown cells of *Synechocystis* PCC 6803. Polarographic measurements of both PS II-mediated O_2 evolution and PS I-mediated photoinhibition of respiratory O_2 uptake (in the presence of 10 μM diuron) were carried out sequentially in the same assays at a chlorophyll equivalent layer density of 0.7 μg cm^{-2}. The spectra were recorded using actinic intermittent illumination of 1 s light flashes with 20 s dark intervals and, in the case of PS II activity measurements, under a weak continuous background light at λ > 700 nm. The spectral half-width of the actinic beam was 3 nm, and its intensity was <0.2 nE cm^{-2} s^{-1}. The spectra are normalized to the maximal activities.

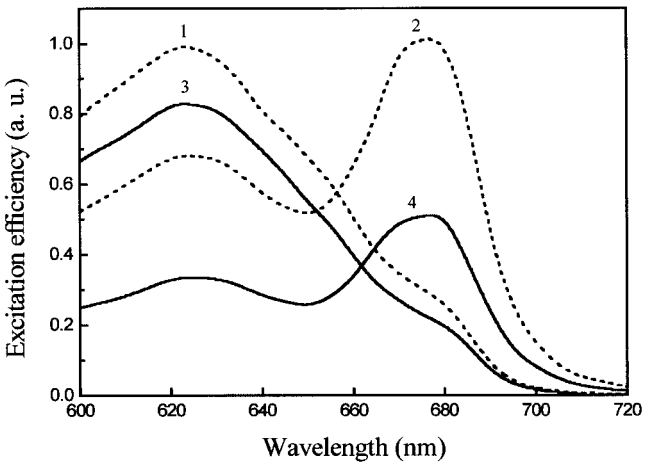

FIGURE 2: Spectral dependence of relative excitation efficiency for PS I and PS II in *Synechocystis* PCC 6803. The efficiency was calculated from the data in Table 1 and Figure 1 as a product of the number of competent reaction centers and optical cross section for photoreaction. Curves: (1) WL-grown cells, PS II; (2) WL-grown cells, PS I; (3) RL-grown cells, PS II; (4) RL-grown cells, PS I.

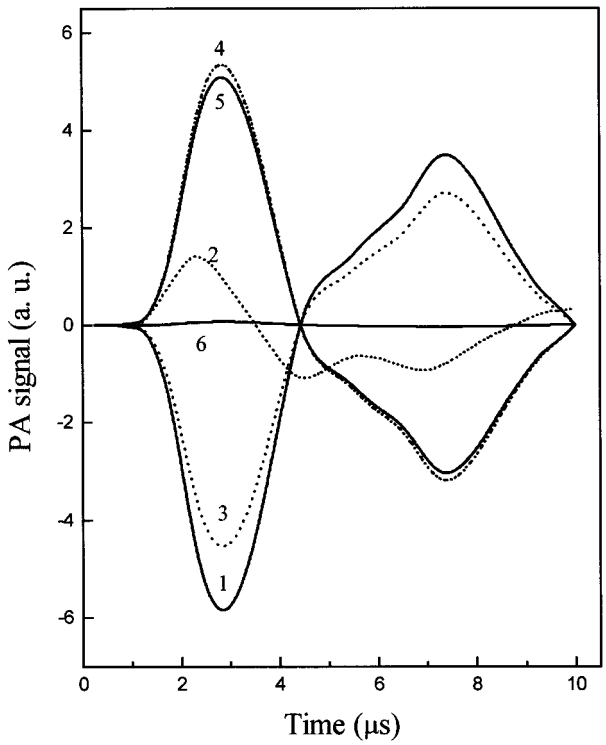

FIGURE 3: Pulsed, time-resolved photoacoustic signals in a typical experiment on *Synechocystis* PCC 6803. RL-grown cells in 10 mM Hepes buffer, pH = 7.2, OD_{680} = 0.15, pulse energy ~2 μJ cm^{-2} at 680 nm: (1) cells, 4 °C; (2) cells under saturating background light, 4 °C; (3) cells, 25 °C; (4) cells under saturating background light, 25 °C; (5) carbon ink solution of the same OD_{680} in the same medium, 25 °C; (6) carbon ink solution, 4 °C. All curves are averages of 256 repetitions at 1 Hz (curves 1 and 3) or 10 Hz (curves 2 and 4−6) laser pulse frequency.

the reference ink solution and photochemically inactive centers closed by a strong background light.

In the measurements of intact cells, the internal reference peak-to-peak signal of closed reaction centers showed a significant deviation from the ink reference at low temperatures (Figure 3, curve 2), similar to that previously reported by Bruce and Salehian (*8*). The thermal diffusion in the cell

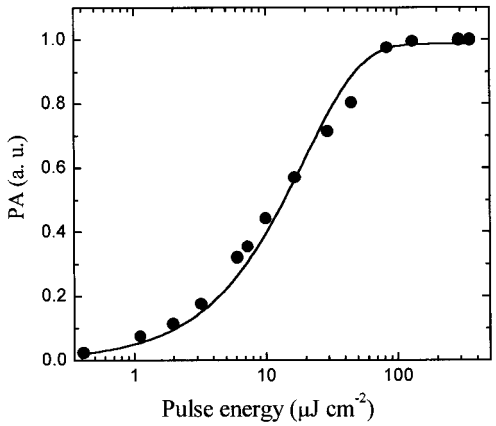

FIGURE 4: Laser pulse energy saturation curve of the photoacoustic signal for WL-grown cells of *Synechocystis* PCC 6803 at 4 °C. The volume contraction signal was measured at a time of zero crossing by the internal reference signal at saturating background light (see curve 2, Figure 3). Each point is an average of 256 to 32 repetitions (from low to high laser pulse energy at 680 nm) at 1 Hz frequency. The fit is the cumulative one-hit Poissonian with σ = 185 Å^2 that corresponds to 80 chlorophyll molecules.

matrix allows it to thermally expand until cooled by the surrounding water. Thus, this heterogeneous artifact depends on the cell size. It will occur only when the thermal relaxation time of the absorbent is longer than the resolution time of the PA detection system. A correction for the cell artifact required use of the eqs 8 and 9 to obtain the thermodynamic parameters as described in Materials and Methods. A global analysis program was written which used all the time-dependent PA data in these equations. A plot of the efficiency or volume versus time then showed when and if these values were constant. The use of all the time data increased confidence in the quoted values.

The pulse saturation curve of the volume contraction signals at 4 °C using 680 nm photons (Figure 4) was fit with a cross section σ of 185 Å^2 that is close to the value of ~190 Å^2 for PS I units estimated by polarographic measurements (Table 1) and corresponds to an effective antenna size of 80 ± 5 chlorophyll molecules.

Photoacoustic data were obtained for both the external and internal references and samples excited at 625 and 680 nm over the range of 0−25 °C. The product of water compressibility κ and PA signal, corrected for the cell artifact, versus the thermal expansion coefficient of water was fit to a straight line with standard deviation ~5% (Figure 5). The slopes were used to estimate enthalpy changes, and the intercept of the sample plot at the temperature of the maximum density of the solution ($\alpha = 0$) was used to obtain the volume change of reaction centers. The reference ink PA signal at 25 °C was used to calibrate the enthalpy and volume changes per absorbed photon.

Table 2 summarizes the thermodynamic characteristics obtained for two cultures of *Synechocystis* PCC 6803 measured at 625 and 680 nm, the spectral maxima of phycobilisomes and chlorophyll *a*. Basically, the PA technique does not distinguish the origin of the charge separation. As shown in Table 2, the estimated volume contraction of reaction centers excited in the spectral region of the phycobilisome band was ~2 times smaller than those excited in the chlorophyll band of the same sample. Energy storage

Table 2: Thermodynamic Characteristics of Intact Cells of *Synechocystis* 6803[a]

	$\lambda_{ex} = 625$ nm			$\lambda_{ex} = 680$ nm		
cells	ΔV, Å^3	ES, %	ES, eV/$h\nu$	ΔV, Å^3	ES, %	ES, eV/$h\nu$
WL grown	-11 ± 1	58 ± 5	1.15 ± 0.1	-21 ± 2	75 ± 10	1.37 ± 0.2
RL grown	-10.5 ± 0.5	50 ± 9	1.0 ± 0.2	-21 ± 1	72 ± 7	1.3 ± 0.15

[a] Data are the averages ± SE for $n = 3-5$. Volume change ΔV was measured at 4 °C and calculated relative to the carbon ink reference at 25 °C with a correction for the cell artifact. Energy storage (ES) was calculated as described in Materials and Methods by a global analysis of the data in the temperature range from 4 to 25 °C. Data obtained at 625 nm were corrected to the excess excitation energy.

Table 3: Thermodynamic Parameters of the Photoinduced Charge-Transfer Reactions in PS I and PS II in the Intact Cells of *Synechocystis* 6803 Compared to the Isolated Complexes

	E_A[a] at 625 nm		E_A[a] at 680 nm					
sample	PS I	PS II	PS I	PS II	ΔV_I, Å^3	ΔH_I, eV	ΔV_{II}, Å^3	ΔH_{II}, eV
WL cells	0.41	0.59	0.79	0.21	-26.5 ± 3	-0.33 ± 0.2	0 ± 3	-0.91 ± 0.2
RL cells	0.30	0.70	0.71	0.29	-28.5 ± 2	-0.31 ± 0.2	-3 ± 2	-1.06 ± 0.2
PS I trimer					-26 ± 2[b]	-0.39 ± 0.1[b]		
apo-PS II core							-3 ± 0.5[c]	-1.15 ± 0.1[c]
							-9 ± 1[d]	-0.9 ± 0.1[d]

[a] The fractions of absorbed energy E_A for each photosystem were estimated from Figure 2. The volume changes ΔV and enthalpy ΔH for the individual reactions are the fit of the data in Table 2 using the contributions of parameters of PS I and PS II at 625 and 680 nm to solve the system of two equations with two unknowns. [b] Data from ref *24*. [c] Data from ref *25*, pH 9. [d] Data from ref *25*, pH 6.

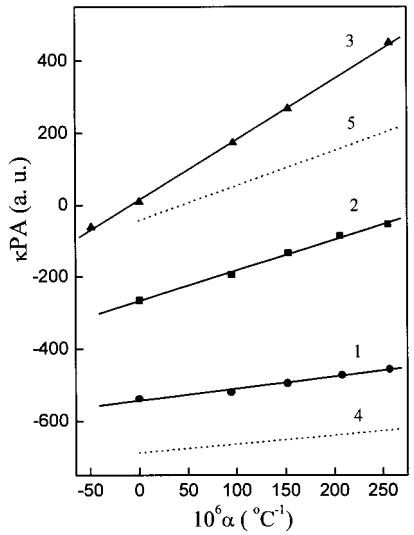

FIGURE 5: Photoacoustic signal times compressibility of water versus the thermal expansion coefficient of water for *Synechocystis* PCC 6803 cells and the carbon ink reference. Data are corrected for the cell artifact as described in Materials and Methods. RL-grown cells in 10 mM Hepes buffer, pH = 7.2, pulse energy ~2 μJ cm^{-2}, OD = 0.17 ± 0.01 at both 625 and 680 nm: (1) cells, 680 nm; (2) cells, 625 nm; (3) ink reference of the same OD; (4) the fit of the PS I signal at 680 nm; (5) the fit of the PS II signal at 680 nm. Each point is an average of 256 to 1024 repetitions at 1 Hz (curve 1) or 10 Hz (curves 2 and 3) laser pulse frequency.

per quantum was also consistently larger in the latter spectral region. However, there was not so much difference between the thermodynamic parameters of WL- and RL-grown cells, which provided different PS I/PS II ratios. Obviously, the wavelength dependence of the volume changes and enthalpy in the cells varies with the significant difference of these parameters for PS I and PS II. Using the data on spectral distribution of the excitation efficiency for PS I and PS II at 625 and 680 nm (Figure 2) and assuming a linear contribution of each to the observed values of volume changes and energy storage per absorbed quantum, it is possible to estimate the individual thermodynamic parameters for the charge separation in PS I and PS II. Table 3 shows the results of such fit, indicating very significant differences between the parameters for PS I and PS II. The volume changes and enthalpy were estimated to be -27 ± 3 Å^2 and -0.33 ± 0.2 eV for PS I, contrasting sharply with the values of -2 ± 3 Å^2 and -1 ± 0.2 eV for PS II. Invariability of the volume changes in response to the PS I/PS II ratio of the cells is direct evidence of a small value of this parameter for PS II. The rather large error of our calculated values of thermodynamic parameters, particularly that of energy storage, was caused by accumulated errors in the determination of the relevant factors by differing methods under differing experimental conditions.

DISCUSSION

According to the known data on kinetics and energetics of photosynthetic reactions (*1*−*4*), in the microsecond time window, separated charges should be stabilized mainly in states $Y_Z^{\bullet}P_{680}Q_A^-$ and $P_{700}^+F_{AB}^-$ or $P_{700}^+Fd^-$. Photosynthetic reaction centers produce upon photoexcitation both a negative photoacoustic signal of the volume contraction and a positive signal of fast heat emission. The former is most likely due to electrostriction, which can be an internal probe of the dielectric coefficient surrounding charges in the reaction center proteins and of their local compressibility (*15*, *17*). Previously, the volume contraction of bacterial reaction centers has been estimated to vary from -12 to -35 Å^3 (*13*−*16*) but most likely is -28 Å^3 (*17*). In oxygenic photosynthesis studies, the only previously reported value is -20 Å^3 for a PS I preparation from *Synechocystis* (*9*).

The present in vivo PA data confirm our results on the isolated reaction centers in vitro (*24*, *25*) that PS I and PS II strongly differ in the volume changes in the microsecond time window. Taking into account the action spectra and the change in molar ratio of PS I/PS II in *Synechocystis* 6803 (Figures 1 and 2, Table 1), one expects equal excitation of PS I and PS II at 625 and 680 nm. A 2-fold difference of the contraction signals in the cells excited at these wavelengths (Figure 5) implies a larger contraction of the PS I

center (Table 3). The contraction signal excited at 680 nm is mainly from PS I as shown by the effective antenna size of ~80 chlorophylls (Figure 4). The same antenna size has been reported for the isolated PS I core complexes from *Synechocystis* 6803 (*24*, *26*).

The fit of individual contributions of each photosystem to the observed values of volume changes (Table 2) from data in Figure 2 revealed −27 and −2 Å^3 for PS I and PS II (Table 3), respectively. A much smaller ΔV in PS II compared to PS I was also observed in the isolated core complexes in vitro (Table 3) (*25*). The small contraction of PS II reaction centers is very likely due to the fast electron transfer from Y_Z^- to P_{680}^+ and possible proton emission (*4*) canceling the charges of the pair (for a detailed discussion, see ref *25*).

In contrast to the contraction signal, the thermal photoacoustic signal is temperature-dependent and allows estimation of the energy storage and enthalpy in the microsecond time range from the ratio of slopes of the κPA vs α plot for sample and references between 0 and 25 °C (Figure 5).

From the excitation energy of P_{680}* and P_{700}* and the known data on the redox potential differences in the states $Y_Z^{\bullet}P_{680}Q_A^-$, +0.97/−0.08 V (*27*, *28*), and $P_{700}^+F_{AB}^-$, +0.49/−0.54 V (*3*) and excitation energy of P_{680}* and P_{700}*, the free energy of these reactions in vivo is −0.77 and −0.74 eV, respectively. If a contribution of entropy to these reactions is assumed to be zero, as often done, then the expected energy storage in both PS II and PS I should be ~58% of the trap energy or ~1.05 eV per absorbed quantum. This value has been reported by Delosme et al. (*9*) in a photoacoustic study of spinach PS II heavy particles and PS I preparations from *Synechocystis*. However, even though these authors, unlike earlier studies (*6*−*8*), considered the contribution of the volume change, the experimental conditions in their PA measurements were probably not optimal. In particular, the extremely high chlorophyll concentrations (OD_{675} ~ 7−20 mm^{-1}) used in the measurements of Delosme et al. (*9*) will distort the PA signal and significantly change the thermal expansion properties of the medium. This is evidenced by the record of positive instead the expected negative PA signal for the PS I particles under saturating background illumination at 0 °C (see Figure 2 in ref *9*).

The fit of the individual contribution of each photosystem to the observed values of energy storage per absorbed quantum in the cells (Table 3) indicated ~80% and ~45% per trap for PS I and PS II, respectively. Similar values of the thermal efficiency were found in the isolated PS I and PS II complexes in vitro (*24*, *25*). Note that the thermal efficiency of PS I on the millisecond time scale is ~40% (*11*, *12*). The enthalpies for the formation of states $P_{700}^+F_{AB}^-$ from P_{700}* and $Y_Z^{\bullet}P_{680}Q_A^-$ from P_{680}* in vivo were estimated to be about −0.3 and −1 eV, respectively. Comparison of these values with the free energies of the reactions indicates a significant contribution of the apparent entropy changes $T\Delta S$, +0.4 and −0.24 eV for the formation of ion radical pairs in PS I and PS II, respectively (Figure 6). We refer to this as an apparent entropy because the free energy may be different in an unrelaxed state of the protein (*17*). Likewise, a positive entropy change has been recently found in the primary reaction of bacterial reaction centers (*17*) and PS I trimers (*24*) that was assigned to the release of counterions from the reaction center surfaces when the charge transfer

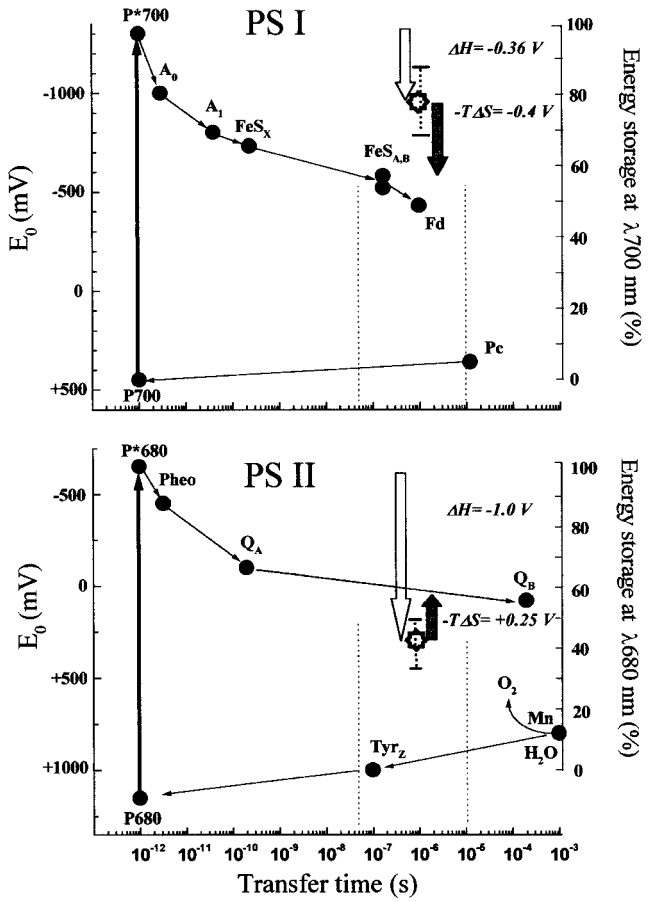

FIGURE 6: Energetic and kinetic scheme of PS I and PS II. Dashed lines show the time window of the PA measurements. Asterisks with error bars are the thermal efficiency in this time window of PS I and PS II. White arrows show the observed values of the enthalpy changes for the formation of the states $P_{700}^+F_{AB}^-$ and $Y_Z^{\bullet}P_{680}Q_A^-$. Dark arrows show the calculated contribution of the entropy changes to the free energy of the charge transfer, as shown as E_0 on the left axis in the figure.

cancels the dominant opposite charges at the interfaces. Unlike PS I and bacterial centers, the entropy of electron transfer in PS II is negative, which is normal for charge formation in solution (*29*). The electron-transfer reaction in PS II is associated with proton transfer favored by a more polar environment in the complex. For a detailed discussion see the preceding paper (*25*). Thus the protein contributes to the thermodynamics of electron-transfer processes. Our method of canceling the cell or heterogeneous artifact now allows accurate PA measurement on whole cells, opening a broad vista of investigations. The artifact itself may contain valuable information on cell size and water content.

ACKNOWLEDGMENT

We are grateful to Dr. G. J. Edens for useful discussions. We thank Irene Zielinski-Large for valuable technical assistance.

REFERENCES

1. Nugent, J. H. A. (1996) *Eur. J. Biochem. 237*, 519−531.
2. Golbeck, J. H. (1994) in *The Molecular Biology of Cyanobacteria* (Bryant, D. A., Ed.) pp 319−360, Kluwer Academic Publishers, Dordrecht, The Netherlands.
3. Brettel, K. (1997) *Biochim. Biophys. Acta 1318*, 322−373.

4. Diner, B. A., and Babcock, G. T. (1996) in *Oxygenic Photosynthesis: The Light Reactions* (Ort, D. R., and Yocum, C. F., Eds.) pp 213−247, Kluwer Academic Publishers, Dordrecht, The Netherlands.
5. Braslavsky, S. E., and Heibel, G. E. (1992) *Chem. Rev. 92*, 1381−1410.
6. Nitsch, C., Braslavsky, S. E., and Schatz, G. H. (1988) *Biochim. Biophys. Acta 934*, 201−212.
7. Mullineaux, C. W., Griebenow, S., and Braslavsky, S. E. (1991) *Biochim. Biophys. Acta 1060*, 315−318.
8. Bruce, D., and Salehian, O. (1992) *Biochim. Biophys. Acta 1100*, 242−250.
9. Delosme, R., Béal, D., and Joliot, P. (1994) *Biochim. Biophys. Acta 1185*, 56−64.
10. Delosme, R., Olive, J., and Wollman, F.-A. (1996) *Biochim. Biophys. Acta 1273*, 150−158.
11. Cha, Y., and Mauzerall, D. (1992) *Plant Physiol. 100*, 1869−1877.
12. Charlebois, D., and Mauzerall, D. (1999) *Photosynth. Res. 59*, 27−38.
13. Arata, H., and Parson, W. (1981) *Biochim. Biophys. Acta 636*, 70−81.
14. Malkin, S., Churio, M. S., Shochat, S., and Braslavsky, S. E. (1994) *J. Photochem. Photobiol. 23B*, 79−85.
15. Mauzerall, D., Gunner, M. R., and Zhang, J. W. (1995) *Biophys. J. 68*, 275−280.
16. Puchenkov, O. V., Kopf, Z., and Malkin, S. (1995) *Biochim. Biophys. Acta 1231*, 197−212.
17. Edens, G. J., Gunner, M. R., Xu, Q., and Mauzerall, D. (2000) *J. Am. Chem. Soc. 122*, 1479−1485.
18. Boichenko, V. A., Klimov, V. V., Mayes, S. R., and Barber, J. (1993) *Z. Naturforsch. 48c*, 224−233.
19. Boichenko, V. A. (1998) *Photosynth. Res. 58*, 163−174.
20. Arnaut, L. G., Caldwell, R. A., Elbert, J. E., and Melton, L. A. (1992) *Rev. Sci. Instrum. 63*, 5381−5389.
21. Porra, R. J., Thompson, W. A., and Kriedemann, P. E. (1989) *Biochim. Biophys. Acta 975*, 384−294.
22. Aizawa, K., Shimizu, T., Hiyama, T., Satoh, K., Nakamura, Y., and Fujita, Y. (1992) *Photosynth. Res. 32*, 131−138.
23. Fujita, Y. (1997) *Photosynth. Res. 53*, 83−93.
24. Hou, J.-M., Boichenko, V. A., Wang, Y.-C., Chitnis, P. R., and Mauzerall, D. (2001) *Biochemistry 40*, 7109−7116.
25. Hou, J.-M., Boichenko, V. A., Diner, B. A., and Mauzerall, D. (2001) *Biochemistry 40*, 7117−7125.
26. Rögner, M., Nixon, P. J., and Diner, B. A. (1990*) J. Biol. Chem. 265*, 6189−6196.
27. Vass, I., and Styring, S. (1991) *Biochemistry 30*, 830−839.
28. Krieger, A., Rutherford, A. W., and Johnson, G. N. (1995) *Biochim. Biophys. Acta 1229*, 193−201.
29. Feitelson, J., and Mauzerall, D. (1996) *J. Phys. Chem. 100*, 7698−7703.

BI010374K